ACS Sustainable Chemistry & Engineering

pubs.acs.org/journal/ascecg

Research Article

Continuous Flow Microbial Flow Cell with an Anion Exchange Membrane for Treating Low Conductivity and Poorly Buffered Wastewater

Ruggero Rossi, Gahyun Baek, Pascal E. Saikaly, and Bruce E. Logan*

Cite This: *ACS Sustainable Chem. Eng.* 2021, 9, 2946–2954

Read Online

ACCESS | Metrics & More | Article Recommendations | Supporting Information

ABSTRACT: Maximum power densities of wastewater-fed microbial fuel cells (MFCs) are limited by low buffer capacities and conductivities. To address these challenges, a continuous flow MFC was constructed using a thin flow channel and an anion exchange membrane (AEM) in a novel configuration. The electrodes were separated only by a thin AEM (~100 μm), reducing the solution resistance while facilitating transport of hydroxide ions from the cathode into the anolyte (no catholyte). The flow-MFC produced 1.34 ± 0.03 W m^{-2} using an artificial wastewater specifically designed to have a low buffer capacity (alkalinity of 360 mg L^{-1}), compared to only 0.37 ± 0.01 W m^{-2} using a more typical cubic-shaped MFC. Internal resistance (R_{int} = 34 ± 1 mΩ m^2) was 83% lower than that of the cubic MFC (202 ± 2 mΩ m^2) due to the better mitigation of pH imbalances between the electrodes by using the AEM and zero-gap electrodes. Performance was benchmarked against a higher buffer concentration (50 mM) solution which showed that the maximum power density with additional buffering increased to 2.88 ± 0.02 W m^{-2}. These results show that MFCs designed for selective hydroxide ion transport will enable improved power production even in low conductivity and poorly buffered solutions such as domestic and industrial wastewater.

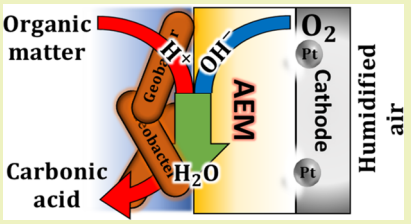

KEYWORDS: *microbial fuel cell, wastewater, pH imbalance, power density, anion exchange membrane*

INTRODUCTION

Low maximum power densities produced by microbial fuel cells (MFCs) have contributed to their limited applications for domestic wastewater treatment. Maximum power densities (PD_{max}) of MFCs treating domestic wastewaters have not exceeded 1.0 W m^{-2}, compared to much greater power densities in well-buffered media and higher solution conductivities (σ > 5 mS cm^{-1}) of PD_{max} = 1.36 ± 0.20 W m^{-2} (n = 24) to 7.1 ± 0.4 W m^{-2}.[1,2] The concentration of organic matter can be a factor for solutions with a chemical oxygen demand (COD) below ~100 mg L^{-1},[3] but maximum performance is low even for wastewater with higher COD concentrations. For example, PD_{max} was only 0.52 ± 0.02 W m^{-2} using domestic wastewater with CODs higher than 300 mg L^{-1}.[4] The specific substrate used in an MFC can impact power production[1] but just increasing the substrate concentration will not increase power if performance is limited by the buffer.[5] For example, addition of 3 g L^{-1} of acetate to a domestic wastewater did not increase the MFC power density (PD_{max} = 0.281 ± 0.007 W m^{-2}).[6] Tests with wastewater having a COD of 9968 ± 32 mg L^{-1} also produced only 0.38 W m^{-2} despite a higher solution conductivity (4.0 ± 0.1 mS cm^{-1}) compared to typical domestic wastewater (~1−1.5 mS cm^{-1})[7,8] Thus, increasing the COD and conductivity of a media will not increase the MFC performance if the buffer capacity of the solution is low. The highest PD_{max} reported to date for domestic wastewater is 0.8 W m^{-2}, which was obtained using a novel Fe−N−C air cathode catalyst in static (fed-batch) conditions in a brush anode, laboratory-scale cubic-type MFC.[9,10] This was larger than that using wastewater with a Pt/C catalyst of 0.4 ± 0.03 W m^{-2} but was still 42% lower than 1.36 ± 0.20 W m^{-2} (n = 24)[1] which was typically produced using the same cell configuration with a well-buffered solution such as 50 mM phosphate buffer (PB).

The low buffer capacity of wastewater limits PD_{max} in MFCs to a greater extent than solution conductivity.[11,12] For example, increasing the PB concentration from 12.5 to 100 mM increased the current density of a graphite anode by >420%, compared to only 15% by adding sodium chloride to match the solution conductivity of the 100 mM phosphate buffer solution (PB).[13] The low buffer capacity primarily impacts anode performance. Organic matter in wastewater is oxidized to volatile fatty acids such as acetate for current generation, which can acidify the anode biofilm. The oxidation of acetate generates 8 mol of protons for each mole of acetate consumed

Received: December 18, 2020
Revised: January 5, 2021
Published: February 8, 2021

(8 mol of e^- transferred), balanced by the release of 8 mol of hydroxide ions at the cathode, according to:[13−15]

$$CH_3COO^- + 4H_2O \rightleftharpoons 2HCO_3^- + 8e^- + 7H^+ \quad (1)$$

$$O_2 + 4e^- + 2H_2O \rightleftharpoons 4OH^- \quad (2)$$

In a typical MFC with an anode−cathode spacing of around 1 cm, charge is not balanced by the transfer of protons and hydroxide ions but instead by other ions present in solution at higher concentrations (Na^+, Cl^-, and HPO_4^{2-}).[11,16,17] Thus, at the anode, protons are generated but not removed from the electrode surface, causing the local anode pH to drop, decreasing the biofilm activity, and lowering the current density. Increasing the buffer capacity of the wastewater reduces pH changes and increases the performance of the anode and therefore power densities,[18−21] for example, from 0.21 to 0.48 W m^{-2} by adding a 50 mM PB to brewery wastewater[19] or from 0.32 ± 0.01 to 1.03 ± 0.06 W m^{-2} for the fermented sludge.[21] However, adding phosphate or salts into wastewater is not a practical approach for wastewater treatment. Instead, changes are needed to the reactor configuration to avoid the development of a low pH in the anode biofilm.[5,13]

In this study, we developed an MFC design to overcome the limitations of low buffer capacity and low conductivity typical of many wastewaters by several design changes that all combined to achieve effective hydroxide ion transport from the cathode to the anode and avoid cation transport into the cathode. These design changes consisted of a thin flow-through anode chamber to reduce concentration gradients near the anode, designing the cells to have only a thin membrane between the anode and cathode acting as a solid electrolyte to minimize solution resistance, and an anion exchange membrane (AEM) to drive hydroxide ion transport (rather than controlling cation transport) (Figure 1). Previous membrane electrode assembly (MEA) designs have focused on using cation exchange membranes (CEMs) or separators to enhance proton transport from an anode to the cathode; however, due to the high concentrations of other cations in solutions (Na^+ and K^+), likely these species were transported by the CEM to the cathode to balance electron transfer.[16,22]

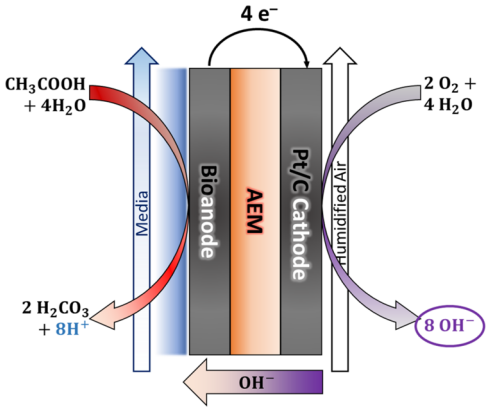

Figure 1. Schematic of the ion transport in the flow-MFC with the AEM. The cathode reaction is balanced by release of hydroxide ions which are the only ion species next to the cathode. The AEM can selectively transport the hydroxide ions from the cathode to the anode to balance the transport of negative electrons in the opposite direction.

The key advancement in the new design here is that it facilitates rapid hydroxide ions away from the cathode to control anode pH more effectively. Humidified air was pumped in the cathode chamber to provide water needed for the generation of hydroxide ions from the oxygen reduction reaction at a pH > 5,[23] avoiding the need for bulk water transport toward the cathode and thus a catholyte and the presence of other ions in it. Selective hydroxide ion transport can improve performance as both charge (electron transfer from the anode to cathode) and pH are balanced by hydroxide ions moving from the cathode to the anode, rather than cations (instead of protons) from the anode to the cathode. Using an AEM can also minimize salt precipitation and fouling in the cathode as ions which can precipitate as salts at high pH are not transported into the cathode by the electric field. The close anode−cathode spacing further minimizes the impact of solution conductivity on the resistance.[24] We investigated the MFC performance using artificial wastewater (aWW) with a low buffer capacity for over 30 days and benchmarked its performance against a typical cube-type MFC design that has been extensively tested with higher buffer concentrations and different substrates. To avoid anode chamber clogging, plastic spacers were used in the anode chamber to allow flow of the media through the anode chamber while maintaining close electrode spacing.

MATERIALS AND METHODS

Construction and Operation of the Flow Cell. The flow cell (Figure S1) was made of two HDPE endplates with separate solution inlets and outlets with threaded connectors drilled into the plates. The anode and cathode chambers were formed by silicon gaskets (7 cm^2 cross sectional area), and the two plates were compressed together so that the anolyte solution was flowing through the anode chamber and only humidified air was pumped through the cathode chamber. The anode chamber was modified from a previous design to have a more open structure and avoid clogging by solids in wastewater using two plastic spacers (S1.5, 30PTFE-625P, Dexmet Corp.) in the anode chamber between the end plate and the anode electrodes.[2] The cathode chamber was similarly constructed to allow air flow, with the electrodes and spacers compressed between the end plates (Figure S1). The empty bed volume of each chamber was approximately 4.45 mL, with the two chambers separated by only an AEM (Selemion, AMV-N, 106 ± 1 μm thick with an ion exchange capacity of 1.85 mmol g^{-1}, Asahi Glass, Co., Tokyo, Japan). The reactors were operated in duplicate at 30 °C with the anolyte (500 mL) recirculated through the MFC at 10 mL min^{-1} (theoretical hydraulic retention time, HRT = 27 s), with a variable external resistance (R_{ext}) in the circuit. Air in the cathode chamber was first humidified by pumping it through a 500 mL distilled water solution. Then the air in the head space was pumped past the cathode at 0.5 mL min^{-1} to provide enough water for the oxygen reduction reaction (ORR). Exhaust air was bubbled in 250 mL of distilled water to avoid back diffusion of gas into the cathode chamber.

The anode was made of two layers of a hydrophilic carbon cloth (ELAT—hydrophilic plain cloth, Fuel Cell Store, USA) heat treated at 450 °C in a muffle furnace for 30 min prior to inoculation.[25] The cathode was a four-layer PTFE wet-proofed carbon cloth (Fuel Cell Store, USA) with a Pt/C (10%) catalyst. Pt loading was 0.5 mg cm^{-2}, and the Pt/C: ionomer (quaternary 1,4-diazabicyclo-[2.2.2]-octane (DABCO) polysulphone (QDPSU)) ratio was 10:1. After electrode fabrication, the cathode and AEM were cold-pressed at 1000 kg cm^{-2} for 10 min (Carver Press, Carver Inc., IN) resulting in the final MEA used in the MFC. Titanium foils were used as current collectors in both anode and cathode chambers.

Typical domestic wastewaters have an alkalinity of 50−200 mg L^{-1}, equivalent to 1−4 mM of PB.[7] Thus, aWW was specifically designed for these tests to have a low buffer capacity and conductivity similar to

https://dx.doi.org/10.1021/acssuschemeng.0c09144
ACS Sustainable Chem. Eng. 2021, 9, 2946−2954

the composition of typical wastewater from the Pennsylvania State University Wastewater Treatment Plant (alkalinity of 360 mg L^{-1} and conductivity of 1.4 mS cm^{-1}) (Table S1). Due to the COVID-19 pandemic, we were not able to routinely collect domestic wastewater for further tests after those with the aWW, and the low number of students on campus during this period would have decreased the strength of the wastewater to values that can adversely impact power production.[26] The aWW contained sodium acetate (1.0 g L^{-1}) and $CaCO_3$ 0.36 g L^{-1}; KCl 0.045 g L^{-1}; NaCl 0.415 g L^{-1}; NH_4Cl 0.1 g L^{-1}; K_3PO_4 0.011 g L^{-1}; $MgSO_4$ 0.1 g L^{-1}, with a final COD of 773 ± 27 mg L^{-1}. This COD was only slightly higher than that previously obtained from the primary effluent collected at the Pennsylvania State University Wastewater Treatment Plant (between 500 and 650 mg L^{-1}).[27] The solution pH was adjusted to 7.5 ± 0.1 with 1 M HCl, and the final conductivity was 1.4 mS cm^{-1}. The solution was used immediately or stored in the fridge (4 °C) for no more than two days to avoid variations in the buffer capacity due to release of CO_2. The aWW was amended with 12.5 mL L^{-1} of a concentrated trace mineral solution and 5 mL L^{-1} of a vitamin solution. The turbidity of the solution was compared with that of aWW by registering a spectrum from 700 to 350 nm with a UV-1800 UV−vis spectrophotometer (Shimadzu, USA) using distilled water as a blank (Figure S2). The performance in aWW was compared with that in a typical PB 50 mM (PB 50 mM: Na_2HPO_4 4.58 g L^{-1}; NaH_2PO_4 H_2O 2.45 g L^{-1}; NH_4Cl 0.31 g L^{-1}; KCl 0.13 g L^{-1}) with a final conductivity of 6.9 mS cm^{-1} and pH of 7.0 ± 0.1. PB was amended with 12.5 mL L^{-1} of a concentrated mineral solution and 5 mL L^{-1} of a concentrated vitamin solution and sodium acetate 2 g L^{-1}.[28]

The carbon cloth anodes were acclimated in a cubic MFC (28 mL internal volume) at +200 mV versus the standard hydrogen electrode (SHE) using an air cathode as a counter electrode and a Ag/AgCl reference electrode (RE) (all potentials reported here vs SHE). The 28 mL volume reactor was inoculated with effluent solution from other operating MFCs mixed with fresh media until current densities larger than 2 A m^{-2} were obtained, and then, only fresh PB was used. The solution was replaced once a day. The spacing between the carbon cloth anode and cathode in the cubic reactor used only for acclimation was 4 cm. Acclimation in such a reactor allowed the solution to not be replaced too often and avoided excessive intrusion of oxygen in the reactor that could have limited anode performance.[29−31] At the end of the acclimation period, when stable peak current densities were obtained, the anodes were transferred to the flow-cell MFCs.

Coulombic efficiency (CE) was calculated as previously described based on the ratio between the total amount of Coulombs generated and the amount of COD consumed.[32] COD was measured using high range COD test tubes (Hach Co., Loveland, CO). Dissolved oxygen concentration was monitored using an optic fiber nonconsumptive oxygen probe (NeoFox, Ocean Optics Inc., Dunedin, FL).

Tests Using Cubic MFCs to Benchmark Performance of the Flow Cells. Cubic MFCs were constructed as previously described[10] and used here to benchmark the performance of the flow cell using this low buffer capacity and low conductivity aWW to a commonly used MFC design. The cubic MFC had a single cylindrical inner volume of 28 mL and an electrode spacing between the carbon brush and the cathode of ∼0.7 cm, lower than the 4 cm distance used during the carbon cloth anode acclimation to avoid the high solution resistance due to a larger spacing. The anode was a carbon brush electrode with the graphite bristles (2.5 cm × 2.5 cm) wound between two Ti wires. A carbon brush was used in this study to compare the cubic MFC performance with the flow-MFC due to the lower performance of carbon felt electrodes in the cubic MFC design.[33] Carbon brushes were heat treated at 450 °C for 30 min as previously described[25] and were inoculated with MFC effluents from another operating MFC fed with sodium acetate (1 g L^{-1}) in PB 50 mM. Once stable operation was obtained following inoculation, only fresh PB medium was used and the reactors were acclimated for more than 4 months. These acclimated MFCs were then fed with the same aWW used in the flow tests. The reactors were acclimated at low external resistance as previously described[34] for more than one week before polarization tests to minimize the occurrence of power overshoot (Figure S4).

Electrochemical Measurements. Anode performance was investigated using linear sweep voltammetries (LSVs). The anode potential was left for 2 h at open circuit potential (OCP) and then scanned from OCP to +300 mV at a scan rate of 0.1 mV s^{-1}. Prior to the LSV, a quick electrochemical impedance spectroscopy (EIS) (from 100 kHz to 500 Hz, 5 mV amplitude, 10 points s^{-1}, ≈25 s $scan^{-1}$) was conducted at the OCP to determine the solution resistance (R_Ω) between the RE and anode, and the electrode potentials were corrected accordingly.[35] Electrodes and whole cell performance were investigated in terms of specific resistance (anode resistance, R_{an}; cathode resistance, R_{cat}; internal resistance, R_{int}) and using the electrode potential slope method.[24]

Single cycle polarization tests were conducted on the flow-MFCs by varying the external resistance at set intervals of time (20 min) unless otherwise noted. The reactors were left for 2 h at OCP, and then, R_{ext} was decreased from 1000 to 500, 200, 100, 75, 50, 30, 20, and 10 Ω after replacing the electrolyte with fresh media. The voltage (U) drop was recorded by a computer-based data acquisition system (VMP3, Biologic, France). Single cycle polarization tests were conducted on the cubic MFCs fed with aWW by varying the external resistance from 2000 to 100 Ω at set intervals of time (20 min) after leaving the cell disconnected for 2 h. Current density (j) and PD were calculated from the current (i) and power (P) defined as $P = iU$ by normalizing the MFC cross-sectional area of the chambers (A = 7 cm^2).[36] At the end of the polarization test, a fast EIS (from 100 kHz to 500 Hz, 5 mV amplitude, 10 points s^{-1}, ≈25 s $scan^{-1}$) was conducted at the OCP to calculate the reactor R_Ω for the flow-MFC. For the cubic MFC, the solution resistance between the anode and cathode and the RE was measured with EIS and used to correct the anode and cathode potential as previously described.[35]

Microbial Community Analysis. The anodic microbial community in the duplicate reactors was characterized with Illumina amplicon sequencing. The carbon cloth was removed at the end of the experiment and stored in RNAlater solution (Thermo Fisher Scientific, USA) prior to DNA and RNA extraction using the FastDNA kit (MP Biomedicals, USA) and RNeasy PowerMicrobiome kit (Qiagen, Germany). The extracted RNA was treated with the DNase Max kit (Qiagen, Germany) to ensure removal of DNA in the samples.

Archaeal and bacterial 16S rRNA gene V4 sequencing libraries were prepared by a custom protocol based on an Illumina protocol (Supporting Information). The resulting amplicon libraries were purified using the standard protocol for Agencourt Ampure XP Beads (Beckman Coulter, USA). Sequencing libraries were prepared from the purified amplicon libraries using a second PCR (Supporting Information).

The purified sequencing libraries were pooled in equimolar concentrations and diluted to 2 nM. The samples were paired end sequenced (2 × 300 bp) on a MiSeq (Illumina, USA) using a MiSeq reagent kit v3 (Illumina, USA) following the standard guidelines for preparing and loading samples on MiSeq. Forward and reverse reads were trimmed, merged, and dereplicated following clustering. Taxonomy was assigned to OTU abundances. The results were analyzed in R v. 4.0.2 (R Core Team, 2017) through the RStudio IDE using the ampvis package v.2.6.4.[37]

RESULTS AND DISCUSSION

Flow-MFC Performance with Wastewater. The flow-through MFC with the AEM produced 1.34 ± 0.03 W m^{-2} after 4 days of operation with aWW. A polarization test was conducted on the reactor by changing the external resistance during continuous operation after 5 days (Figure 2A). The PD_{max} in the polarization test slightly decreased to 1.24 ± 0.04 W m^{-2} compared to continuous operation but the MFC internal resistance, calculated from the slope of the polarization curve, was only 34 ± 1 mΩ m^2 (Figure 2B). The solution

https://dx.doi.org/10.1021/acssuschemeng.0c09144
ACS Sustainable Chem. Eng. 2021, 9, 2946−2954

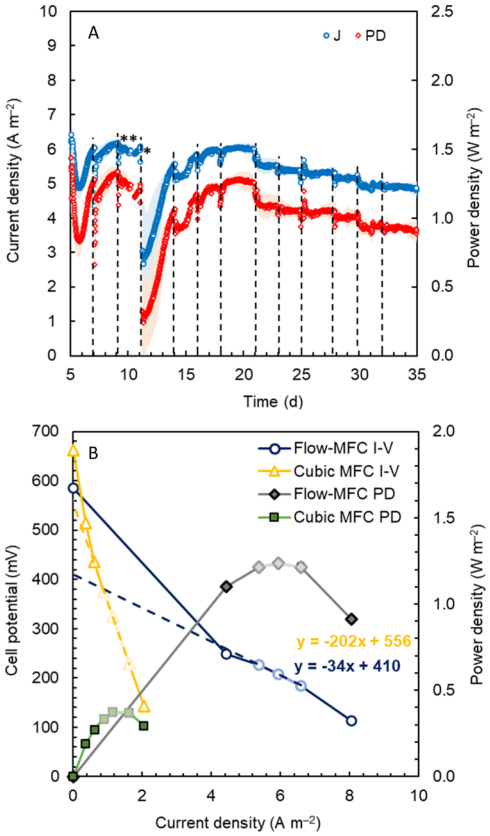

Figure 2. (A) PD and current density (J) during acclimation in the flow cell with 50 Ω external resistance and wastewater. The dashed lines indicate when the solution was replaced with a new media. The asterisks represent the polarization tests. (B) Comparison of maximum PD in the flow-through MFC and in the cubic MFC with a brush anode and AC cathode with the same cross-sectional area (7 cm^2). The OCP value for the flow-MFC was obtained from the polarization test reported in Figure S3.

resistance, obtained using EIS, was found to contribute only 4% to the total internal resistance (1.29 ± 0.04 mΩ m^2). For comparison, an MFC with 1 cm electrode spacing would have had a solution resistance of 102 mΩ m^2, calculated based on the solution conductivity (1.4 mS cm^{-1}). Thus, using compact configuration with zero-gap electrode spacing allowed minimal impact of a medium with a low conductivity on the solution resistance. Previous studies have showed that due to the low solution conductivity of wastewater, the solution resistance in a cubic MFC fed with domestic wastewater can account up to 39% of the internal resistance, greatly reducing power production using this reactor configuration.[24,35]

The flow-through MFC PD_{max} was more than 3× larger than that obtained in a 28 mL state-of-the-art cubic MFC of 0.38 ± 0.01 W m^{-2} with a brush anode and air cathode (7 cm^2), fed with aWW. PD_{max} of the cubic MFC here was similar to that previously reported using domestic wastewater (~0.3−0.4 W m^{-2}).[10,21,24,27,38,39] A similar performance was obtained with the aWW, and these previous studies using actual wastewaters demonstrated that the performance of wastewater fed with MFCs was primarily affected by the buffer capacity and not the substrate (acetate or organic matter in wastewater). The OCP of the flow-through MFC (585 ± 8 mV) was obtained from the single cycle polarization test reported in Figure S3. This value was lower than that obtained with the cubic MFC (663 ± 2 mV) likely due to the intrusion of oxygen in the anode during the 2 h at OCP in the single cycle polarization tests. The anolyte pH was stable during the whole experiments and was not affected by the operational time of the MFCs. The COD concentrations here with acetate were only slightly larger than the CODs with actual domestic wastewaters in previous studies (439 ± 55 and[3] 545 ± 5 mg L^{-1}[40]).

The low PD_{max} of the cubic MFC was due to its larger internal resistance compared to the flow-MFC. The cubic-MFC internal resistance was 202 ± 2 mΩ m^2 with a large solution resistance of 51 ± 1 mΩ m^2 contributing to ~25% of R_{int}. Anode (61 ± 2 mΩ m^2) and cathode (89 ± 4 mΩ m^2) resistances were similar to those previously reported using domestic wastewater with similar reactor configurations.[24] The sum of R_{an} and R_{cat} in the cubic MFC (150 mΩ m^2) was much larger than the whole R_{int} of the flow MFC (34 ± 1 mΩ m^2) due to the favored transport of the hydroxide ions from the cathode to the anode, which reduced the acidification and thus diffusion resistance of the anodic reaction, diminishing the overall electrode resistance. Previous studies have showed that brush electrodes outperform carbon cloth anodes;[33,35] thus, the difference obtained here could not be due to the different electrode materials used in the flow-MFC (carbon cloth) and the cubic MFC (brush anode). These results show that the use of the aWW here produced results similar to those with actual wastewaters.

Stability of Flow-MFC Performance. The stability of MFC performance over time is critical for MFC application treating wastewaters. Reactor performance was therefore examined for a month as previous studies have shown significant deterioration in performance during the first month of operation.[38,41] The flow-MFC performance was relatively stable over a month of operation (Figure 2A), with only a 28% decrease in the PD from 1.3 ± 0.1 W m^{-2} (day 9) to 0.97 ± 0.03 W m^{-2} (day 35). This decrease was much less than the 65% reduction previously observed for cubic MFCs lacking an AEM (from 0.30 ± 0.02 to 0.11 ± 0.01 W m^{-2} over one month).[38] As it was not possible to monitor the individual electrode potentials in the flow MFC with a RE due to its thin spacing, it was not clear which electrode was responsible for the largest drop in the performance over time. However, many previous studies have shown that degradation in power production was primarily due to a reduction in cathode performance,[42] with salt precipitation identified as the main reason for this decline.[29] The ORR at the cathode generates hydroxide ions from the reduction of oxygen that results in local alkalinization of the cathodic environment. If charge balance is maintained by positive ion transport into the cathode structure (Ca^{2+} and Mg^{2+}), then at high pH, salts will precipitate on the electrode if the buffer capacity is too low to maintain a pH close to neutral. No salt precipitation was visible from the photos of the AEM side of the MEA cathode (Figure S12), likely due to the close spacing between the electrodes that allowed to neutralize any pH imbalance across the membrane. The presence of a biofilm on the cathode can further adversely impact performance by limiting the transport of protons and hydroxide ions between the electrodes.[43] In the flow-MFC, since there is no space between the membrane and the cathode in the MEA configuration, the biofilm development on the cathode was inhibited (photos of the anode and MEA cathode are reported in the Supporting Information), and the pH imbalances between the electrodes were minimized by the selective transport of hydroxide ions through the AEM.

https://dx.doi.org/10.1021/acssuschemeng.0c09144
ACS Sustainable Chem. Eng. 2021, 9, 2946−2954

Small precipitates were found between the different spacers used in the anode chamber (Figure S13) due to the high solid content of the aWW. In future studies, a single thicker spacer could be used to increase the void volume of the reactor while minimizing solid accumulation. The AEM avoided the transport of cations to the cathode, limiting their role in precipitation as salts on the catalyst and thus likely increasing the electrode durability.[44]

The average CE over the whole duration of the experiment was 103 ± 30%, likely due to the low air flux past the cathode and the AEM, which limited the oxygen intrusion in the anolyte during normal operations. The average COD removal was 10 ± 3% over the first month of operation with the aWW.

Flow-MFC Performance with an Acetate−PB Medium. The performance of the flow-MFC was also examined using a 50 mM PB solution to benchmark its performance relative to previous designs in well-buffered solution. The PD_{max} was 3.1 ± 0.1 W m^{-2} with this well-buffered solution (Figure 3A). This PD was about half that previously obtained

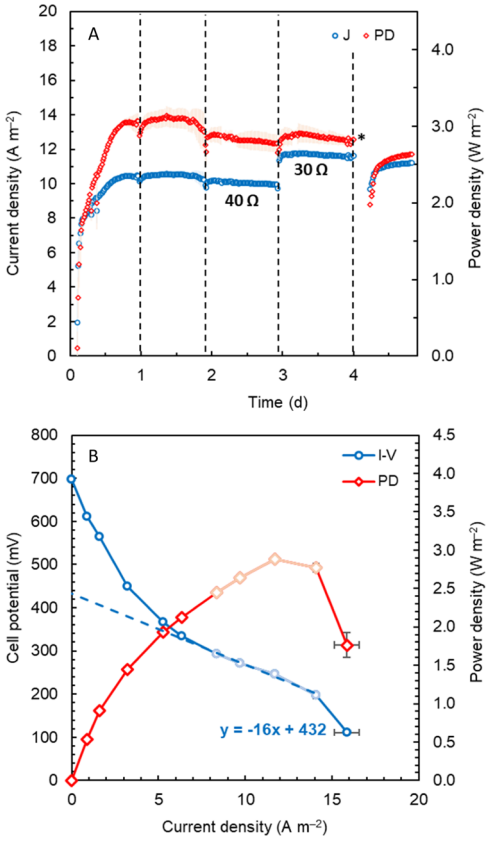

Figure 3. (A) PD and current density (J) during acclimation in the flow cell with 20 Ω external resistance and acetate in PB medium. The dashed lines indicate when the solution was replaced with a new media. *Polarization test. (B) PD and polarization curve of the MFCs. The dashed lines represent the linearization of the data in the maximum power region.

(5.7 ± 0.4 W m^{-2}) using the same medium but with flow driven through a felt anode[2] likely due to the lower surface area available of the two layers of carbon cloth for biofilm development compared to carbon felt. We also operated the reactor with a single carbon cloth layer instead of two layers, and power was further reduced to 1.8 ± 0.1 W m^{-2} with erratic performance in terms of current production (Figure S8), indicating that reducing the anode surface area adversely impacted power production in this novel configuration.[45]

The current density of the two carbon cloth layers in the assembled flow-MFC with the AEM (10.5 ± 0.2 A m^{-2}) was 38% larger than the peak current density of the same two carbon cloth layer anode obtained in the cubic MFC in LSV tests with a large anode cathode spacing (4 cm) and no AEM (7.6 ± 0.6 A m^{-2}) (Figure S7). This higher current of the same anode in the flow-MFC configuration was due to the enhanced transport of hydroxide ions through the AEM compared to the cubic reactor with 4 cm spacing, where local anodic and cathodic pH were not balanced. It has been previously shown that the anode resistance is due to a combination of kinetic and mass transport resistance, with the diffusion of protons from the electrode responsible for the latter.[46] Thus, mitigating the development of low pH at the anode electrode can diminish the electrode resistance and allow the production of higher current density compared to configuration where the pH imbalance is not mitigated. The whole cell MFC internal resistance from polarization tests (Figure 3B) that includes anode, cathode, and solution resistance (16.5 ± 1.3 mΩ m^2) was similar to the anode resistance alone when tested in a 4 cm cube reactor with LSV (R_{an} = 15.6 ± 0.2 mΩ m^2), suggesting that the AEM and the small electrode spacing reduced the impact of diffusion resistance on the anode, diminishing its resistance. Unfortunately, the compact MFC configuration did not allow to measure the individual anode and cathode potentials against a reference, thus only the whole cell internal resistance was calculated from the slope of the polarization curve.

PD_{max} decreased and stabilized after two days of operation at 2.9 ± 0.1 W m^{-2} likely due to the development of preferential flow paths within the anode chamber (Figure 3A).[2] Decreasing R_{ext} from 40 to 30 Ω further increased the maximum current density over the cycle to 11.8 ± 0.3 A m^{-2}, with negligible impact on the power generation, suggesting that the MFC was operating near its maximum performance.

Oxygen intrusion did not appear to affect MFC performance as dissolved oxygen was quickly removed from the solution recirculated through the anolyte chamber (Figure S9). The highest dissolved oxygen concentration was measured immediately following replacement of the medium and depleted to below detection limits after around 2 h of operation. A low oxygen crossover to the anode resulted in a relatively high and stable CE of 80 ± 5% over the initial cycles.

The PD_{max} measured four days after acclimation in 50 mM PBS was 2.88 ± 0.02 W m^{-2} at 11.7 ± 0.1 A m^{-2}, similar to that obtained during continuous operation with a fixed external resistance (Figure 3B). The solution resistance calculated from EIS was only 0.91 ± 0.01 mΩ m^2, less than 6% of the overall internal resistance, while the anode and cathode were contributing to the remaining 15.6 mΩ m^2. This internal resistance was more than double than that obtained using an MFC configuration with a flow-through felt anode (7.2 ± 0.6 mΩ m^2),[2] suggesting that anodes with a high surface area should be used to maximize performance with flow-MFCs if anode chamber clogging is not a concern. At high current densities, MFC performance was limited by mass-transport, as suggested by the steep decrease in potential for current densities larger than 15 A m^{-2} (Figure 3B). Unfortunately, the compact design used in this study did not allow direct monitoring of the individual electrode potentials with a RE.

https://dx.doi.org/10.1021/acssuschemeng.0c09144
ACS Sustainable Chem. Eng. 2021, 9, 2946−2954

Therefore, it was not clear if mass-transport limitations were due to anodic or cathodic reactions.

After the polarization test, the MFC performance was subsequently reduced for a short period of time (Figure 3A, day 4). It was not clear if this temporary decrease was due to prolonged operation at OCP and low current densities (>3 h) or the low R_{ext} used for the last point of the polarization curve (10 Ω) and the resulting high current density. However, the initial performance was recovered after less than a day in continuous operation mode (Figure 3A).

Microbial Community Analysis. The microbial community analysis based on DNA conducted after one month of operation in aWW revealed that most abundant bacterial population colonizing the carbon cloth anodes belonged to the genus *Geobacter* (Figure 4). These results are in line with many

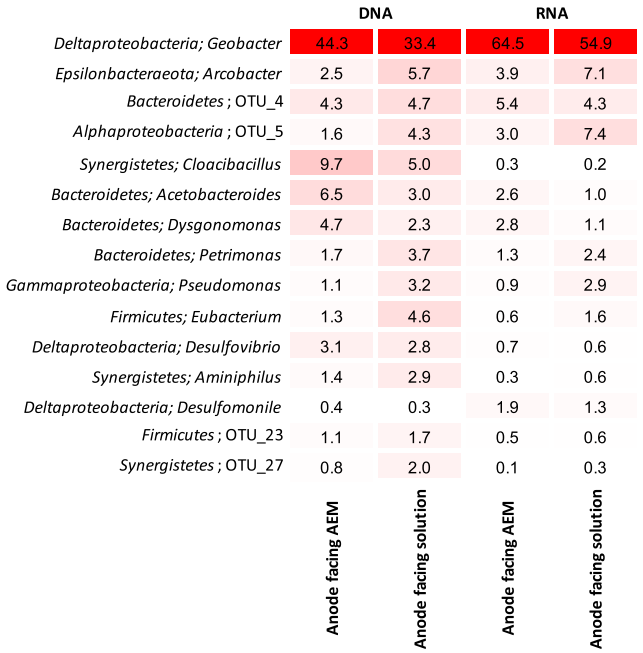

Figure 4. Heatmap of the 15 most abundant genera averaged between the duplicate samples.

previous studies where members of the genus *Geobacter* were the most abundant microorganisms involved in exogenous electron transfer.[9,47] However, some studies have shown a predominance of other microorganisms, for example, *Proteiniphilum acetatigenes* in an MFC with a small electrode spacing that produced up to 5.9 ± 0.5 W m^{-2} with a highly saline anolyte (12.5 mS cm^{-1}).[48] The relative abundance of *Geobacter* decreased by increasing the distance between the anode and the AEM. For example, the relative abundance of *Geobacter* was 44% in the carbon cloth closer to the AEM and decreased to 33% in the carbon cloth layer further from the membrane. The second most prevalent genus identified on the electrodes was *Arcobacter*, with a relative abundance around 1 order of magnitude lower than *Geobacter*. Archaea were not detected in our samples. Similarly, microbial community analysis based on RNA revealed that members of *Geobacter* were the most active microorganisms on the anodes and that its activity decreased by moving the electrodes further from the AEM.

Implications on the Use of Compact Reactors with the AEM for Wastewater Treatment. Using membranes in MFCs has largely been avoided due to early studies showing that the presence of a CEM hot pressed on a cathode was detrimental for the MFC performance.[49] For example, using a CEM (Nafion) in a MEA air cathode with a flat carbon electrode decreased PD_{max} from 0.49 ± 0.02 to 0.26 ± 0.01 W m^{-2} using glucose as a substrate in 50 mM PB.[49] Based on many subsequent studies since then, this reduced performance was attributed to the transport of other cations than protons (0.1 μM), such as Na^+ or K^+ that were more concentrated in solution (~0.1 M).[15,50] When species other than protons or hydroxide ions are transported between the electrodes to balance charge, the anode pH would decrease and the cathode pH would increase, resulting in a higher internal resistance and lower voltage output.[16,50] Thus, the use of an AEM with zero spacing against the cathode and no catholyte, where the localized hydroxide ion concentration would be higher than in the bulk solution, mitigated the increase in cathode pH and more effectively balanced the pH in the anolyte.

Reducing the MFC internal resistance is the most effective strategy to increase the performance of air-cathode MFCs. Anode, cathode, solution, and membrane (if present) resistances are the only components of the R_{int} of MFCs.[51] The anode resistance is primarily affected by the diffusion of protons from the electrode to the bulk solution, and it has been previously shown that increasing the buffer capacity increases the anode performance by reducing the overall anode resistance and increasing the limiting current density.[5,13] Cathode resistance is due to the kinetics of the ORR[5,52] while solution and membrane resistances represent the resistance in the transport of ions between the electrodes.[35]

Performance degradation over time has been another major drawback limiting the use of MFCs to treat wastewater.[42] The maximum power densities of wastewater-fed MFCs can decrease over time mainly due to air cathode fouling.[29,41,42] It has been shown in several studies that salt precipitation, due to the localized pH increase within the cathode structure, decreased the electrode conductivity and reduced the available catalytic surface area.[29,43] For example, salt precipitation increased the cathodic charge transfer resistance by ~53% in a 28 mL MFC with a brush anode and air cathode in a well-buffered solution.[29] Biofouling is another important contributor to performance degradation of an MFC, with the cathode resistance 37% larger when a thick biofilm was developed on the cathode.[29,42] To date, the most effective method to recover initial cathode performance is removing the electrode and cleaning it by scraping off the biofilm, prior to immersing it in a concentrated acid solution to remove salt deposits.[27,42] This method would require frequent interruptions in MFC operation, generate large volumes of waste acid solutions, increase work requirements for treatment plant operators, and therefore prohibit the use of these MFCs in treatment plants. Thus, MFC configurations that improve power production must also need to provide stable performance over time and not require frequent maintenance by plant operators.

In this study, using an AEM and a close electrode spacing allowed minimization of the MFC internal resistance and produced the highest PD ever reported for an MFC fed with a media with low buffer capacity, similar to that of domestic wastewater. The ORR at the cathode produced the hydroxide ions that, in the absence of a catholyte, are transported through the AEM to the anolyte, where they neutralize the protons produced by the substrate oxidation. The absence of the catholyte also limited the detrimental precipitation of salts within the electrode, increasing the long-term performance of

https://dx.doi.org/10.1021/acssuschemeng.0c09144
ACS Sustainable Chem. Eng. 2021, 9, 2946−2954

the MFC. Unfortunately, the high cost of ion exchange membranes (IEMs) could limit their application in wastewater treatment. However, cheaper alternatives such as reverse osmosis membranes have shown comparable resistances to IEMs in a seawater electrolyzer,[53] opening the possibility to use water treatment membranes in MFCs if cost and selectivity trades off.

CONCLUSIONS

A zero-gap anode cathode spacing with an AEM as the only separator between the electrodes minimized the solution resistance, avoided large pH imbalances between the electrodes, and overcame the limitations imposed by low buffer concentrations of wastewaters. The flow-through MFC produced the highest PD (1.34 ± 0.03 W m^{-2}) ever reported in a low conductivity and low buffer capacity solution due to the selective transport of the hydroxide ions produced at the cathode to the anode electrode. The separator assembly in the anode chamber avoided clogging while ensuring a close contact between the electrodes, as shown by the low solution resistance from EIS (1.29 ± 0.04 mΩ m^2). The zero-gap spacing coupled with the selectivity of the AEM limited the deterioration of the MFC performance over time, with the PD_{max} decreasing by only 28% over one month of operation.

ASSOCIATED CONTENT

Supporting Information

The Supporting Information is available free of charge at https://pubs.acs.org/doi/10.1021/acssuschemeng.0c09144.

MFC configuration; turbidity of the aWW solution compared to actual domestic wastewater; single cycle polarization test of the flow-through AEM MFC; cubic MFC performance in terms of power and electrode potentials; anode and the flow-through AEM MFC performance (four figures); oxygen concentration over time in the anolyte during normal operation; photos of the anode and the AEM at the end of the experiment; and average wastewater composition recorded at the Pennsylvania State University Wastewater Treatment Plant (PDF)

AUTHOR INFORMATION

Corresponding Author

Bruce E. Logan − *Department of Civil and Environmental Engineering, The Pennsylvania State University, University Park, Pennsylvania 16802, United States;* orcid.org/0000-0001-7478-8070; Email: blogan@psu.edu

Authors

Ruggero Rossi − *Department of Civil and Environmental Engineering, The Pennsylvania State University, University Park, Pennsylvania 16802, United States;* orcid.org/0000-0002-3807-3980

Gahyun Baek − *Department of Civil and Environmental Engineering, The Pennsylvania State University, University Park, Pennsylvania 16802, United States;* orcid.org/0000-0002-3707-5300

Pascal E. Saikaly − *Biological and Environmental Science and Engineering Division, Water Desalination and Reuse Research Center, King Abdullah University of Science and Technology, Thuwal 23955-6900, Saudi Arabia;* orcid.org/0000-0001-7678-3986

Complete contact information is available at: https://pubs.acs.org/10.1021/acssuschemeng.0c09144

Author Contributions

R.R. and B.E.L. designed research; R.R. performed research; R.R., G.B., P.E.S., and B.E.L. analyzed data and wrote the manuscript before submission.

Notes

The authors declare no competing financial interest.

ACKNOWLEDGMENTS

The authors acknowledge funding by the Environmental Security Technology Certification Program via cooperative research agreement W9132T-16-2-0014 through the US Army Engineer Research and Development Center and funding by the Pennsylvania State University.

REFERENCES

(1) Yang, W.; Kim, K.-Y.; Saikaly, P. E.; Logan, B. E. The Impact of New Cathode Materials Relative to Baseline Performance of Microbial Fuel Cells All with the Same Architecture and Solution Chemistry. *Energy Environ. Sci.* **2017**, *10*, 1025−1033.

(2) Rossi, R.; Wang, X.; Logan, B. E. High Performance Flow through Microbial Fuel Cells with Anion Exchange Membrane. *J. Power Sources* **2020**, *475*, 228633.

(3) Zhang, X.; He, W.; Ren, L.; Stager, J.; Evans, P. J.; Logan, B. E. COD Removal Characteristics in Air-Cathode Microbial Fuel Cells. *Bioresour. Technol.* **2015**, *176*, 23−31.

(4) Wu, S.; He, W.; Yang, W.; Ye, Y.; Huang, X.; Logan, B. E. Combined Carbon Mesh and Small Graphite Fiber Brush Anodes to Enhance and Stabilize Power Generation in Microbial Fuel Cells Treating Domestic Wastewater. *J. Power Sources* **2017**, *356*, 348−355.

(5) Rossi, R.; Hall, D. M.; Wang, X.; Regan, J. M.; Logan, B. E. Quantifying the Factors Limiting Performance and Rates in Microbial Fuel Cells Using the Electrode Potential Slope Analysis Combined with Electrical Impedance Spectroscopy. *Electrochim. Acta* **2020**, *348*, 136330.

(6) Karra, U.; Troop, E.; Curtis, M.; Scheible, K.; Tenaglier, C.; Patel, N.; Li, B. Performance of Plug Flow Microbial Fuel Cell (PF-MFC) and Complete Mixing Microbial Fuel Cell (CM-MFC) for Wastewater Treatment and Power Generation. *Int. J. Hydrogen Energy* **2013**, *38*, 5383−5388.

(7) Rozendal, R. A.; Hamelers, H. V. M.; Rabaey, K.; Keller, J.; Buisman, C. J. N. Towards Practical Implementation of Bioelectrochemical Wastewater Treatment. *Trends Biotechnol.* **2008**, *26*, 450−459.

(8) Sevda, S.; Dominguez-Benetton, X.; Vanbroekhoven, K.; De Wever, H.; Sreekrishnan, T. R.; Pant, D. High Strength Wastewater Treatment Accompanied by Power Generation Using Air Cathode Microbial Fuel Cell. *Appl. Energy* **2013**, *105*, 194−206.

(9) Logan, B. E.; Rossi, R.; Ragab, A. a.; Saikaly, P. E. Electroactive Microorganisms in Bioelectrochemical Systems. *Nat. Rev. Microbiol.* **2019**, *17*, 307−319.

(10) Yang, W.; Logan, B. E. Immobilization of a Metal-Nitrogen-Carbon Catalyst on Activated Carbon with Enhanced Cathode Performance in Microbial Fuel Cells. *ChemSusChem* **2016**, *9*, 2226−2232.

(11) Rittmann, B. E. Ironies in Microbial Electrochemistry. *J. Environ. Eng.* **2017**, *143*, 03117001.

(12) Popat, S. C.; Torres, C. I. Critical Transport Rates That Limit the Performance of Microbial Electrochemistry Technologies. *Bioresour. Technol.* **2016**, *215*, 265−273.

(13) Torres, C. I.; Kato Marcus, A.; Rittmann, B. E. Proton Transport inside the Biofilm Limits Electrical Current Generation by Anode-Respiring Bacteria. *Biotechnol. Bioeng.* **2008**, *100*, 872−881.

(14) Popat, S. C.; Ki, D.; Rittmann, B. E.; Torres, C. I. Importance of OH^- Transport from Cathodes in Microbial Fuel Cells. *ChemSusChem* **2012**, *5*, 1071−1079.
(15) Modin, O.; Fukushi, K.; Rabaey, K.; Rozendal, R. A.; Yamamoto, K. Redistribution of Wastewater Alkalinity with a Microbial Fuel Cell to Support Nitrification of Reject Water. *Water Res.* **2011**, *45*, 2691−2699.
(16) Rozendal, R. A.; Hamelers, H. V. M.; Buisman, C. J. N. Effects of Membrane Cation Transport on pH and Microbial Fuel Cell Performance. *Environ. Sci. Technol.* **2006**, *40*, 5206−5211.
(17) Luo, S.; Fu, B.; Liu, F.; He, K.; Yang, H.; Ma, J.; Wang, H.; Zhang, X.; Liang, P.; Huang, X. Construction of Innovative 3D-Weaved Carbon Mesh Anode Network to Boost Electron Transfer and Microbial Activity in Bioelectrochemical System. *Water Res.* **2020**, *172*, 115493.
(18) Huang, L.; Logan, B. E. Electricity Generation and Treatment of Paper Recycling Wastewater Using a Microbial Fuel Cell. *Appl. Microbiol. Biotechnol.* **2008**, *80*, 349−355.
(19) Feng, Y.; Wang, X.; Logan, B. E.; Lee, H. Brewery Wastewater Treatment Using Air-Cathode Microbial Fuel Cells. *Appl. Microbiol. Biotechnol.* **2008**, *78*, 873−880.
(20) Wen, Q.; Wu, Y.; Zhao, L.; Sun, Q. Production of Electricity from the Treatment of Continuous Brewery Wastewater Using a Microbial Fuel Cell. *Fuel* **2010**, *89*, 1381−1385.
(21) Yang, F.; Ren, L.; Pu, Y.; Logan, B. E. Electricity Generation from Fermented Primary Sludge Using Single-Chamber Air-Cathode Microbial Fuel Cells. *Bioresour. Technol.* **2013**, *128*, 784−787.
(22) Oliot, M.; Galier, S.; Roux de Balmann, H.; Bergel, A. Ion Transport in Microbial Fuel Cells: Key Roles, Theory and Critical Review. *Appl. Energy* **2016**, *183*, 1682−1704.
(23) Zhou, Z.; Pei, Z.; Wei, L.; Zhao, S.; Jian, X.; Chen, Y. Electrocatalytic Hydrogen Evolution under Neutral pH Conditions: Current Understandings, Recent Advances, and Future Prospects. *Energy Environ. Sci.* **2020**, *13*, 3185−3206.
(24) Rossi, R.; Cario, B. P.; Santoro, C.; Yang, W.; Saikaly, P. E.; Logan, B. E. Evaluation of Electrode and Solution Area-Based Resistances Enables Quantitative Comparisons of Factors Impacting Microbial Fuel Cell Performance. *Environ. Sci. Technol.* **2019**, *53*, 3977−3986.
(25) Feng, Y.; Yang, Q.; Wang, X.; Logan, B. E. Treatment of Carbon Fiber Brush Anodes for Improving Power Generation in Air-Cathode Microbial Fuel Cells. *J. Power Sources* **2010**, *195*, 1841−1844.
(26) He, W.; Zhang, X.; Liu, J.; Zhu, X.; Feng, Y.; Logan, B. E. Microbial Fuel Cells with an Integrated Spacer and Separate Anode and Cathode Modules. *Environ. Sci.: Water Res. Technol.* **2016**, *2*, 186−195.
(27) Rossi, R.; Wang, X.; Yang, W.; Logan, B. E. Impact of Cleaning Procedures on Restoring Cathode Performance for Microbial Fuel Cells Treating Domestic Wastewater. *Bioresour. Technol.* **2019**, *290*, 121759.
(28) Cheng, S.; Xing, D.; Call, D. F.; Logan, B. E. Direct Biological Conversion of Electrical Current into Methane by Electromethanogenesis. *Environ. Sci. Technol.* **2009**, *43*, 3953−3958.
(29) An, J.; Li, N.; Wan, L.; Zhou, L.; Du, Q.; Li, T.; Wang, X. Electric Field Induced Salt Precipitation into Activated Carbon Air-Cathode Causes Power Decay in Microbial Fuel Cells. *Water Res.* **2017**, *123*, 369−377.
(30) Kim, K.-Y.; Yang, W.; Logan, B. E. Impact of Electrode Configurations on Retention Time and Domestic Wastewater Treatment Efficiency Using Microbial Fuel Cells. *Water Res.* **2015**, *80*, 41−46.
(31) Chen, S.; Brown, R. K.; Patil, S. A.; Huber, K. J.; Overmann, J.; Schröder, U. Aerobic Microbial Electrochemical Technology Based on the Coexistence and Interactions of Aerobes and Exoelectrogens for Synergistic Pollutant Removal from Wastewater. *Environ. Sci.: Water Res. Technol.* **2019**, *5*, 60−69.
(32) Logan, B. E.; Hamelers, B.; Rozendal, R.; Schröder, U.; Keller, J.; Freguia, S.; Aelterman, P.; Verstraete, W.; Rabaey, K. Microbial Fuel Cells: Methodology and Technology. *Environ. Sci. Technol.* **2006**, *40*, 5181−5192.
(33) Logan, B.; Cheng, S.; Watson, V.; Estadt, G. Graphite Fiber Brush Anodes for Increased Power Production in Air-Cathode Microbial Fuel Cells. *Environ. Sci. Technol.* **2007**, *41*, 3341−3346.
(34) Watson, V. J.; Logan, B. E. Analysis of Polarization Methods for Elimination of Power Overshoot in Microbial Fuel Cells. *Electrochem. Commun.* **2011**, *13*, 54−56.
(35) Logan, B. E.; Zikmund, E.; Yang, W.; Rossi, R.; Kim, K.-Y.; Saikaly, P. E.; Zhang, F. Impact of Ohmic Resistance on Measured Electrode Potentials and Maximum Power Production in Microbial Fuel Cells. *Environ. Sci. Technol.* **2018**, *52*, 8977−8985.
(36) Lu, L.; Gu, J.; Ren, Z. J. Comment on "Unbiased Solar H_2 Production with Current Density up to 23 mA cm^{-2} by Swiss-Cheese Black Si Coupled with Wastewater Bioanode. *Energy Environ. Sci.* **2019**, *12*, 3412−3414.
(37) Albertsen, M.; Karst, S. M.; Ziegler, A. S.; Kirkegaard, R. H.; Nielsen, P. H. Back to Basics - The Influence of DNA Extraction and Primer Choice on Phylogenetic Analysis of Activated Sludge Communities. *PLoS One* **2015**, *10*, No. e0132783.
(38) Rossi, R.; Yang, W.; Zikmund, E.; Pant, D.; Logan, B. E. In Situ Biofilm Removal from Air Cathodes in Microbial Fuel Cells Treating Domestic Wastewater. *Bioresour. Technol.* **2018**, *265*, 200−206.
(39) Zhang, F.; Ahn, Y.; Logan, B. E. Treating Refinery Wastewaters in Microbial Fuel Cells Using Separator Electrode Assembly or Spaced Electrode Configurations. *Bioresour. Technol.* **2014**, *152*, 46−52.
(40) Stager, J. L.; Zhang, X.; Logan, B. E. Addition of Acetate Improves Stability of Power Generation Using Microbial Fuel Cells Treating Domestic Wastewater. *Bioelectrochemistry* **2017**, *118*, 154−160.
(41) Yang, W.; Rossi, R.; Tian, Y.; Kim, K.-Y.; Logan, B. E. Mitigating External and Internal Cathode Fouling Using a Polymer Bonded Separator in Microbial Fuel Cells. *Bioresour. Technol.* **2018**, *249*, 1080−1084.
(42) Zhang, E.; Wang, F.; Yu, Q.; Scott, K.; Wang, X.; Diao, G. Durability and Regeneration of Activated Carbon Air-Cathodes in Long-Term Operated Microbial Fuel Cells. *J. Power Sources* **2017**, *360*, 21−27.
(43) Yuan, Y.; Zhou, S.; Tang, J. In Situ Investigation of Cathode and Local Biofilm Microenvironments Reveals Important Roles of OH^- and Oxygen Transport in Microbial Fuel Cells. *Environ. Sci. Technol.* **2013**, *47*, 4911−4917.
(44) Sugioka, M.; Yoshida, N.; Iida, K. On Site Evaluation of a Tubular Microbial Fuel Cell Using an Anion Exchange Membrane for Sewage Water Treatment. *Front. Energy Res.* **2019**, *7*, 91.
(45) Caizán-Juanarena, L.; Krug, J. R.; Vergeldt, F. J.; Kleijn, J. M.; Velders, A. H.; Van As, H.; Ter Heijne, A. 3D Biofilm Visualization and Quantification on Granular Bioanodes with Magnetic Resonance Imaging. *Water Res.* **2019**, *167*, 115059.
(46) ter Heijne, A.; Schaetzle, O.; Gimenez, S.; Navarro, L.; Hamelers, B.; Fabregat-Santiago, F. Analysis of Bio-Anode Performance through Electrochemical Impedance Spectroscopy. *Bioelectrochemistry* **2015**, *106*, 64−72.
(47) Corbella, C.; Guivernau, M.; Viñas, M.; Puigagut, J. Operational, Design and Microbial Aspects Related to Power Production with Microbial Fuel Cells Implemented in Constructed Wetlands. *Water Res.* **2015**, *84*, 232−242.
(48) Oliot, M.; Etcheverry, L.; Mosdale, A.; Basseguy, R.; Délia, M.-L.; Bergel, A. Separator Electrode Assembly (SEA) with 3-Dimensional Bioanode and Removable Air-Cathode Boosts Microbial Fuel Cell Performance. *J. Power Sources* **2017**, *356*, 389−399.
(49) Liu, H.; Logan, B. E. Electricity Generation Using an Air-Cathode Single Chamber Microbial Fuel Cell in the Presence and Absence of a Proton Exchange Membrane. *Environ. Sci. Technol.* **2004**, *38*, 4040−4046.
(50) Sleutels, T. H. J. A.; Hamelers, H. V. M.; Rozendal, R. A.; Buisman, C. J. N. Ion Transport Resistance in Microbial Electrolysis

https://dx.doi.org/10.1021/acssuschemeng.0c09144
ACS Sustainable Chem. Eng. 2021, 9, 2946−2954

Cells with Anion and Cation Exchange Membranes. *Int. J. Hydrogen Energy* **2009**, *34*, 3612−3620.
(51) Fan, Y.; Sharbrough, E.; Liu, H. Quantification of the Internal Resistance Distribution of Microbial Fuel Cells. *Environ. Sci. Technol.* **2008**, *42*, 8101−8107.
(52) Yin, F.; Hu, P.; Song, C.; Wang, S.; Liu, H. Unveiling the Role of Gas Permeability in Air Cathodes and Performance Enhancement by Waterproof Membrane Fabricating Method. *J. Power Sources* **2020**, *449*, 227570.
(53) Shi, L.; Rossi, R.; Son, M.; Hall, D. M.; Hickner, M. A.; Gorski, C. A.; Logan, B. E. Using Reverse Osmosis Membranes to Control Ion Transport during Water Electrolysis. *Energy Environ. Sci.* **2020**, *13*, 3138−3148.

https://dx.doi.org/10.1021/acssuschemeng.0c09144
ACS Sustainable Chem. Eng. 2021, 9, 2946−2954